

AD-A077 536

NAVAL RESEARCH LAB WASHINGTON DC
MACHINING FLAWS AND THE STRENGTH GRAIN SIZE BEHAVIOR OF CERAMIC--ETC(U)
SEP 79 R W RICE

F/G 11/2

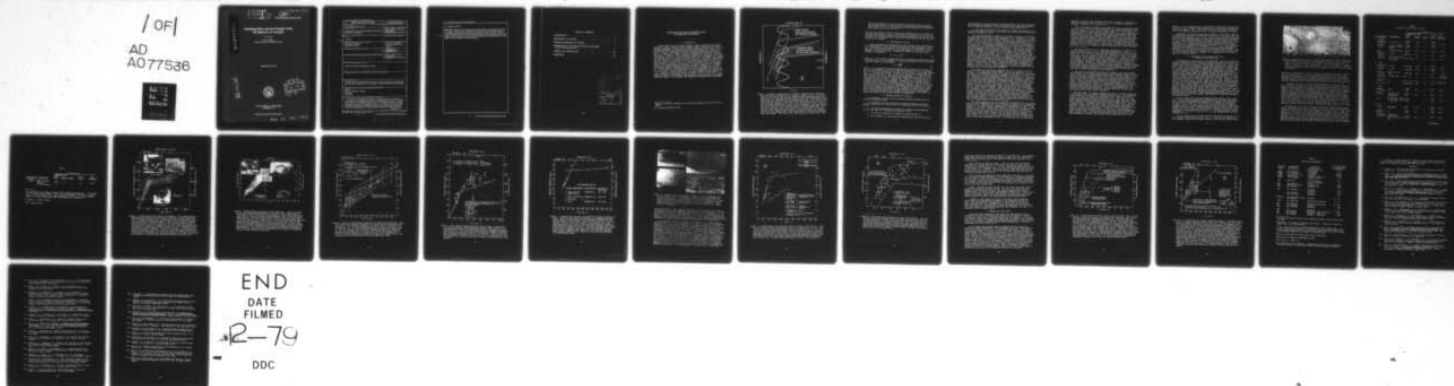
UNCLASSIFIED

NRL-MR-4076

SBIE-AD-E000 335

NL

/OF/
AD
A077536



END
DATE
FILMED

2-79

DDC

LEVEL III

(12) Adeooo 335

NRL Memorandum Report 4076

AD A 077536

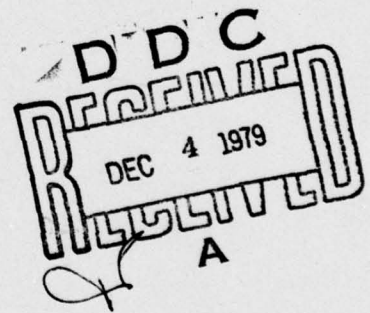
Machining Flaws and the Strength Grain Size Behavior of Ceramics

R. W. RICE

*Ceramics Branch
Material Science and Technology Division*

September 28, 1979

DDC FILE COPY



NAVAL RESEARCH LABORATORY
Washington, D.C.

Approved for public release; distribution unlimited.

79 11 08 081

SECURITY CLASSIFICATION OF THIS PAGE (When Data Entered)

REPORT DOCUMENTATION PAGE		READ INSTRUCTIONS BEFORE COMPLETING FORM
1. REPORT NUMBER NRL Memorandum Report 4076	2. GOVT ACCESSION NO.	3. RECIPIENT'S CATALOG NUMBER (7)
4. TITLE (and Subtitle) MACHINING FLAWS AND THE STRENGTH GRAIN SIZE BEHAVIOR OF CERAMICS	5. TYPE OF REPORT & PERIOD COVERED Interim report on a continuing NRL problem	
6. PERFORMING ORG. REPORT NUMBER		8. CONTRACT OR GRANT NUMBER(s)
7. AUTHOR(s) R. W. Rice	9. PERFORMING ORGANIZATION NAME AND ADDRESS Naval Research Laboratory Washington, DC 20375	
10. PROGRAM ELEMENT, PROJECT, TASK AREA & WORK UNIT NUMBERS NRL Problem 63M05-12 and 63P03-19		11. CONTROLLING OFFICE NAME AND ADDRESS (11) 28
12. REPORT DATE September 28, 1979		13. NUMBER OF PAGES 27
14. MONITORING AGENCY NAME & ADDRESS (if different from Controlling Office) (14) NRL-MR-4076 (12) 28		15. SECURITY CLASS. (of this report) UNCLASSIFIED
16. DISTRIBUTION STATEMENT (of this Report) Approved for public release; distribution unlimited. (18) SBIE (19) AD-E000 335		15a. DECLASSIFICATION/DOWNGRADING SCHEDULE
17. DISTRIBUTION STATEMENT (of the abstract entered in Block 20, if different from Report)		
18. SUPPLEMENTARY NOTES This report serves as a preprint/reprint of the paper by the same title and author that will appear in the Proceedings of Conference on the The Science of Ceramic Machining and Surface Finishing, II.		
19. KEY WORDS (Continue on reverse side if necessary and identify by block number) Strength Grain size dependence of strength Flaw sizes Brittle failure		
20. ABSTRACT (Continue on reverse side if necessary and identify by block number) A model for the strength-grain size dependence of ceramics failing from machining flaws is presented based on the observation that the size of machining flaws (C) shows little or no dependence on grain size. Two regimes of behavior are seen. At finer grain sizes, little or no strength dependence on grain size (G) exists because flaws are $> G$. For large G, the significant decrease of strength with increasing G is attributed by a transition from polycrystalline to either lower single crystal or grain boundary (i.e. bicrystal) fracture energies as the \sim constant (C) becomes (Continues) APPROXIMATE		

DD FORM 1473

1 JAN 73

EDITION OF 1 NOV 65 IS OBSOLETE
S/N 0102-014-6601

SECURITY CLASSIFICATION OF THIS PAGE (When Data Entered)

251 950

LB

20. Abstract (Continued)

A2293 significantly less than the G as G increases. The transition between the two regimes is when C and G are similar. Extensive analysis of strength-grain size data, and more limited directly correlated fractographic data support the proposed model. Spontaneous cracking in non-cubic materials is shown to support the model, but not be an alternate explanation for the transitions seen in machined Al_2O_3 or BeO. This analysis also further supports the observation that machining flaws do not vary greatly with typical variations in machining parameters.

A

TABLE OF CONTENTS

INTRODUCTION	1
MECHANISMS OF FAILURE.	3
PROPOSED MECHANISM OF FAILURE.	3
COMPARISON OF THE STRENGTH GRAIN SIZE MODEL WITH AVAILABLE DATA.	6
SUMMARY AND CONCLUSIONS.	18
REFERENCES.	22

Accession For	
NTIS <input checked="" type="checkbox"/>	
DDC TAB <input type="checkbox"/>	
Unannounced <input type="checkbox"/>	
Justification <input type="checkbox"/>	
By _____	
Distribution/ _____	
Availability Codes	
Dist.	Avail and/or special
A	

MACHINING FLAWS AND THE STRENGTH GRAIN SIZE BEHAVIOR OF CERAMICS

1. Introduction

Single phase as well as some multiphase ceramic polycrystalline bodies, especially those of limited to zero porosity, show a definitive and characteristic dependence of their brittle tensile failure on grain size (G) [1-4].¹ For most materials, such behavior occurs to temperatures of at least a few hundred °C and for many more refractory bodies to temperatures of 1000°C or more. Typically, two regimes of such G dependence of brittle fracture are observed. At larger G , there is typically a significant increase in tensile (or flexure) strength(s) as G decreases. However, as G decreases below some intermediate level, e.g. below 10 to 50 μm , much less or possibly no, increase in S is observed with further decreasing G (fig. 1). The latter regime showing more limited or no increase in S with decreasing G typically gives a non-zero intercept on a Petch plot, i.e. a plot of S versus $G^{-1/2}$. In the past, such non-zero intercepts have often been interpreted as indicating strength control due to microplastic nucleation or growth of cracks [1-3]. However, recent fractographic information shows that this is commonly not the case, that flaws, commonly from machining, are typically the source of failure [2-4]. In the past, it was often assumed that the G dependence of S was due to the flaw size (C) being related to G , i.e. most commonly it was assumed that $C = G$. However, recent fractographic information shows that the size of flaws introduced by machining do not vary much, if at all, with G [5]. Thus, flaws are typically much smaller than large grains and typically much larger than fine grains. This extensive fractographic information thus invalidates

¹Figures in brackets indicate the literature references at the end of this paper.

Note: Manuscript submitted July 6, 1979.

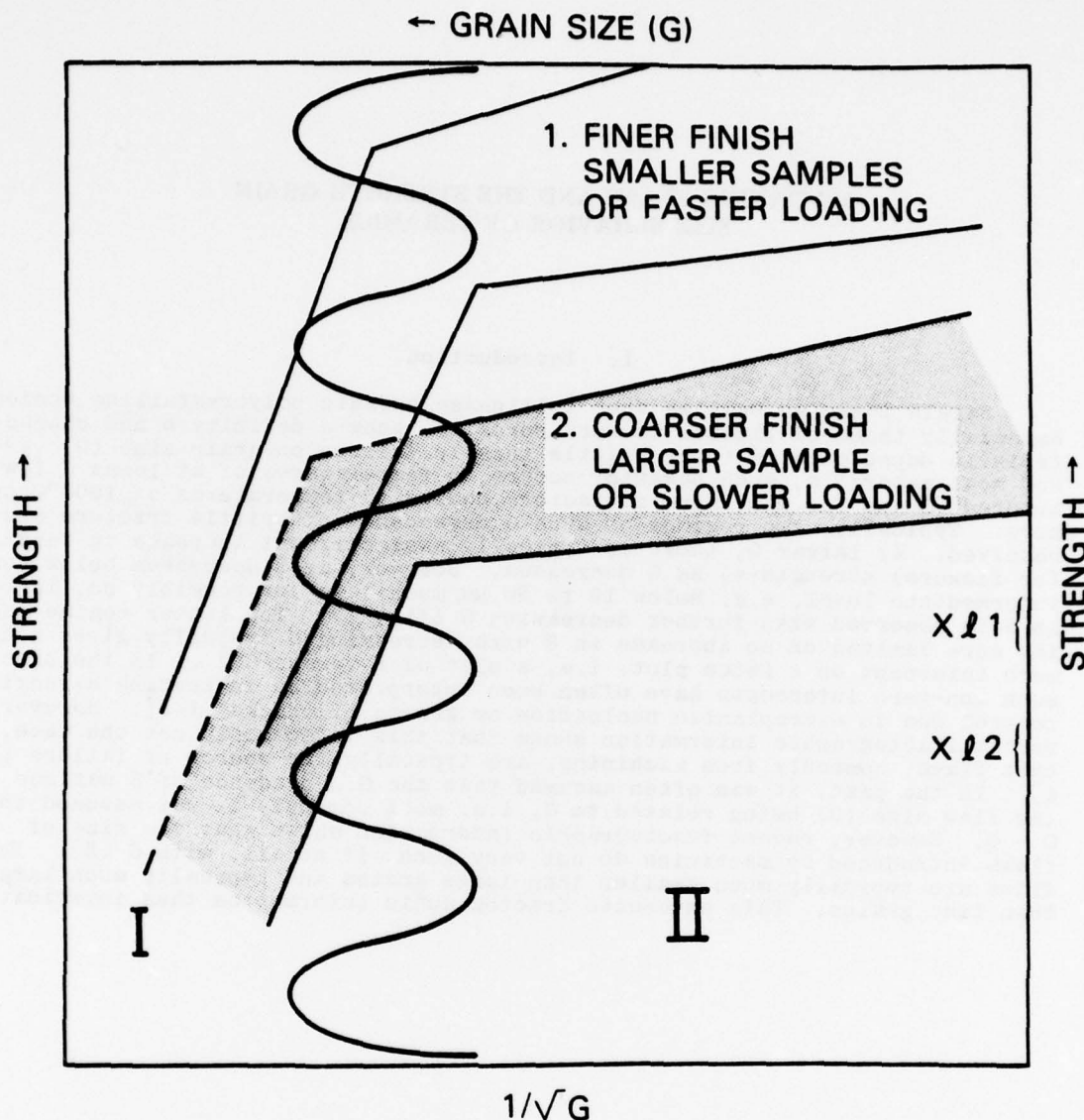


Figure 1. Schematic representation of proposed strength-grain size model. Note that this is divided into two regions. Region I is for larger grain sizes where strength significantly increases with decreasing grain size. Region II is for finer grain sizes where strength shows significantly less, and possibly no, increase with decreasing grain size. The transition between these two regions occurs over a grain size range where the grain and flaw sizes are similar as indicated by the vertical wavy line. The two sets of trends indicated by 1) and 2) are for samples of the same material but having different surface finish, sizes, or testing conditions. There may be an overlap of one or both regions for two such sample sets over the full grain size extent, or partial overlap (as shown), or no overlap. However, it is commonly expected that due to scatter and other factors that there will commonly be at least some degree of overlap in the larger grain size regime. Note also on the right hand side of the figure that

the strength ranges for single crystals of the same material in their weaker orientations with the same set of finishing or testing parameters are indicated for the two sets of polycrystalline samples by 1) and 2) are shown respectively by X/1 and X/2.

the previous explanation for the grain size dependence of brittle failure of ceramics under tensile loading. The purpose of this paper is to review the pertinent fractographic observations on machining flaws and S-G data in order to relate the two together and to discuss the mechanisms of failure that they demonstrate or suggest.

2. Mechanisms of Failure

Before reviewing the fractographic and S-G data and their interrelation, it is appropriate to first briefly review the two basic mechanisms of failure. One mechanism is failure due to microplastic crack nucleation, due to blocking of slip bands or twins by other slip bands or other twins, or more commonly, by grain boundaries. Microplastic failure is typically represented by the equation:

$$S = \sigma_0 + KG^{-\frac{1}{2}} \quad (1)$$

where σ_0 is the stress to activate the slip or twinning phenomena that leads to failure, and K is a constant. The second mechanism, that of flaw failure, typically follows the relationship:

$$S = A \sqrt{\frac{E\gamma}{C}} \quad (2)$$

where A is a geometrical factor associated with the shape of the flaw, and may also be dependent on the size of the flaw relative to that of the specimen, as well as the location of the flaw in the specimen, E is Young's modulus, and γ is the fracture energy. As noted earlier, it has commonly been assumed in the past that C was related to G , commonly $C = G$, implying that one should be able to tell whether the mechanisms implied by eqs. (1) or (2) were operative by plotting S versus $G^{-\frac{1}{2}}$. Equation (1) would result in a straight line with a non-zero intercept at σ_0 , while eq. (2) would result in a straight line with a zero intercept. However, as noted earlier and discussed in detail later, C is generally not related to G so this is not a valid method of separating the two mechanisms. Further, there are other complications such as the fact that the two mechanisms may interact, e.g. slip may aid the growth of pre-existing flaws to grow to a critical size. Also, there can be competition between the two processes such that one may dominate in one grain size region and the other in another grain size regime, with a transition between the two regimes shifting with such parameters as impurities, porosity, and surface finish, e.g. machining.

3. Proposed Mechanism of Failure

Any mechanism of brittle failure of polycrystalline ceramics must address the following factors:

1. Foremost is the fact that failure typically appears to initiate from machining flaws that have little or no dependence on G as noted earlier [5].
2. The observed dependence of strength on surface finish parameters such as grit size [6-9] and machining direction [5,10].
3. The possible dependence of strength on specimen size [5].
4. That strengths of polycrystalline specimens can often extend below

the strengths of single crystals of the same material given the same surface finishing which are tested in those orientations that give lower strength due to favorable orientation of lower fracture energy planes [2,4].

5. The expected interaction or competition between microplastic and brittle mechanisms of failure in materials such as MgO where the former mechanism can be operative [1,2].

The proposed mechanism of tensile (or flexural) failure is as follows. First consider the smaller G regime indicated by II in figure 1, i.e. where strength shows either limited or no dependence of G. Fractography has clearly shown that in this region flaws are typically many grains in size [2-5]. Since E does not depend on G, γ often does not depend significantly on G [2, 4, 11], and the flaws are multi-grained in size and show no relationship to the grain size, no significant dependence of S on G would thus be expected. This absence of any significant G dependence for failure with $C > G$ gives a non-zero intercept on a Petch plot, e.g. figure 1. This is now believed to be the predominant source of non-zero intercepts. The possible limited increase of strength with decreasing G in this region (II) can arise from either of at least two sources. The first source is some possible limited decrease of C with decreasing G [5], e.g. possibly following the limited increase of hardness with decreasing G. A second possible source is the effect of internal stresses, i.e. due to incompatible strains between grains in non-cubic materials or materials that have undergone a phase transformation. Since there are statistical variations of these stresses, as the number of grains encompassed by C decreases, internal stresses can increasingly aid failure. Such effects can begin to occur even when flaws encompass many grains [1,2,4,12]. With C nearly constant, the number of grains encompassed by the flaw increases with decreasing G, which would thus reduce the internal stress effect, and hence increase S.

This leaves the significant dependence of S on G in region I and the reason for the transition between regions I and II of figure 1 to be explained. A key observation is that the transition between these two different regimes of S-G behavior typically appears to occur when $C \sim G$ [2-4, 13]. Two explanations for the significant decrease in strength as G increases so the \sim constant C becomes progressively $< G$ have been considered. The first is that the machining flaws start propagating below the failure stress but are arrested when they encounter the adjacent grains. Failure would thus result when the stress increases to the level to propagate the flaw now the size of the grain in which it has grown, or the size of one or more grain boundary facets for intergranular flaws, into or around the surrounding grains. This mechanism provides a ready explanation for the G dependence of S in region I (fig. 1) since it gives the final flaw size $\sim G$. However, this mechanism leaves unexplained how cracks can grow several fold in size so their increase in stress intensity is greater than the change in fracture toughness on going from a single- to multi-grain crack can be arrested. Further, this mechanism does not explain how polycrystalline bodies with initial flaws similar to those in single crystals of the same material can have strengths similar to, or below, those of the weakest orientation of such crystals when polycrystalline fracture energies are several fold times those for common single- or bi-crystal fracture.

The second explanation for the significant G dependence of S in region I rests on the recognition that for C sufficiently smaller than G flaws would effectively see themselves in a single crystal environment for flaws within grains, or in a grain boundary environment for grain boundary flaws. In the extreme of such cases, failure would then be controlled by the single crystal fracture energy (γ_c) for failure on the easier cleaving or fracture surfaces of the single crystal or the fracture energy (γ_b) for crack propagation along a single grain boundary, e.g. bicrystal fracture energies. γ_c values vary from $\sim 1/3$ to $\sim 1/10$ of typical polycrystalline fracture energy (γ_{pc}) values. γ_b can be anywhere from a fraction, e.g. $1/2$, to 100% of γ_c . Thus, as previously suggested [2,4,14], it is proposed that the significant

increase in strength with decreasing grain size in region I arises from an effective transition from γ_c or γ_B to γ_{pc} as G of different specimens decrease relative to an \sim constant C.

Recent calculations indicate that unless the flaw is a sufficient fraction of G, e.g. 1/3 to 1/2, that propagation will become catastrophic before the crack reaches the grain boundary where a major, if not the total, increase of fracture energy towards γ_{pc} would occur [14]. This transition has been sketched out in some cubic materials based on calculations using the initial flaw size [4,14]. However, some crack growth may also occur [15]. There are also questions of whether the change from γ_c or γ_B to γ_{pc} values is really gradual or possibly a step function. The above noted transition could, in fact, be a result of different more abrupt transitions of individual flaws in different specimens due to varying grain-flaw parameters such as sizes and location [14]. In any event, it appears that the second mechanism, that of a γ transition, applies when C is sufficiently small relative to G, e.g. $C < G/3$, while the first is operative for C larger relative to G, e.g. $C > G/3$.

The above transition in γ is completed at different C/G ratios in different materials, e.g. ~ 1 to 3. This range depends upon a variety of factors such as texture and the orientation dependence of γ within a single grain [14]. The C/G ratio over which this transition occurs can also vary depending on the size, shape, and location of the flaw. Thus, for example, a flaw may be rather shallow but fairly elongated so it crosses into two or three grains, so it probably reached γ_{pc} sooner than a penny shaped flaw of the same depth located entirely within one grain or entirely along one grain boundary. Similarly, a flaw located entirely within a grain, but located adjacent to one grain boundary may have a different transition than a flaw whose ends are well away from the grain boundaries. Internal stresses from thermal expansion anisotropy (TEA) or phase transformation and redistribution of applied stresses due to elastic anisotropy (EA) may also effect the C/G ratios for completing this transition.

Note that the polycrystalline strength in region I can extend below the strengths for the weaker orientation of single crystals having the same surface finish as the polycrystalline materials for several reasons (fig. 1). There are extrinsic causes of this, such as impurities, and porosity. However, there are also intrinsic causes such as failure from grain boundary flaws in materials in which γ_B values are sufficiently below those of γ_c values. Also, internal stresses from phase transformation or TEA can contribute to failure either by adding to the applied stress or by allowing larger machining flaws to form, e.g. by machining flaws linking up with pre-existing cracks from the internal stresses or cracks forming from such stresses during machining operations. Stress concentrations due to EA, which also occurs in cubic materials, may also contribute to lower polycrystalline versus single crystal strengths.

The above model is clearly consistent with all of the observed effects of machining. Thus, for example, grinding perpendicular to the tensile axis of bars generally introduces more elongated and hence more severe flaws whether they are much larger or smaller than G [5]. They also lower the transition because, as noted above, elongated flaws should reach γ_{pc} values sooner because of their interaction with a greater number of grains. Similarly, effects of changing grit size would have the same effect. Again, in a similar fashion, if larger flaws occur in larger bodies, they will lower strengths in both large and fine G bodies and thus give transitions at larger G. Finally, the competition and trade-off between microplastic and flaw failure can also be anticipated. Since slip or twin nucleation of cracks is typically associated with slip bands and/or twins propagating across a single grain, a pre-existing flaw larger than that grain will dominate failure. Thus, entirely brittle failure of materials that can exhibit microplastic failure, such as MgO and CaO should occur for $C > G$.

However, as the C approaches G, the microplastic mechanisms can become competitive so that as flaws become smaller than the grain size, microplastic failure can begin to occur. When flaws are still a sufficient fraction of the G, slip assisted crack growth may be a dominant mechanism of failure.

Subsequent to the authors original discussion of this model, Bradt and colleagues also discussed a similar model in which the fine grain size region was also attributed to $C > G$ [6,]. They, however, attributed the transition and the subsequent larger G region where S depends more extensively on G to a change from machining to "intrinsic" flaws of unspecified character which they apparently felt depended upon G for an explanation of the G dependence of S. Several aspects of the model proposed by the present author were also independently proposed by Rhodes et al [16] who similarly attributed the transition in S-G behavior to $C \sim G$. Also, some aspects of the model were suggested in an earlier review of devitrified glasses by Emrich [17], i.e. a two branch S-G relation depending upon flaw size. Emrich attributes this model to Stookley [17], but the latter reference does not show a definite base for the model, so it appears that it is really more due to Emrich himself.

4. Comparison of the Strength Grain Size Model with Available Data

Considerable S-G data exists in the literature. Much of it lacks definitive characterization of either the surface finishing conditions or the strength test methods, and little fractography has been done. Much of the earlier data does not necessarily show a clear transition for several reasons. First, often only limited G ranges were investigated. Second, much of the data was not plotted in a fashion to clearly show such transitions, e.g. log-log plots which tend to obscure such transitions. Finally, there is also an important experimental difficulty in many materials; namely, variable grain sizes. Thus, for example, bodies such as Al_2O_3 which often readily exhibit exaggerated grain growth may have one large grain at or near the surface in which one or more machining flaws may form. If a flaw forms in or along such a large grain, that flaw is likely to be the source of failure which will then reflect a large, if not total, influence of the size of that large grain. In such cases, plotting S as a function of the average G can be quite misleading. Some have, therefore, plotted strength as a function of the largest G. While this author was one of the first to recognize such possible effects of large grains just inside the machined tensile surface, he has also clearly observed cases where large grains are present, but machining flaws did not form in them (e.g. fig. 2) and hence plotting their strength as a function of the large G is incorrect. This uncertainty of which G is controlling thus leads to substantial scatter in the data and must be considered. Despite these problems, there is still a substantial amount of data which either individually or collectively supports the proposed theory.

Figure 3 shows one of the more complete studies which, in fact, was one of the factors precipitating the development of the model of section 3. Note in figure 3 that the inserted fractographs of fracture initiating flaws clearly show an increase of the strength as G decreases as discussed in the model. Also, note since this is a cubic material in which internal stresses from TEA, or other complications such as those due to phase transformation are not present, one can calculate fracture energies from the indicated flaw sizes. Such calculated fracture energies do, in fact, show a transition from approximately 2 J/m^2 for $C < G$ in good agreement with DCB measurements of γ_c to $\sim 7 \text{ J/m}^2$ for $C > G$ in good agreement with DCB measurements of γ_{pc} .

The only other set of S-G data that has associated fractography with it are the more limited studies of B_4C (fig. 4). Evaluation of earlier B_4C data suggests a transition as shown in figure 4, and the more recent data of

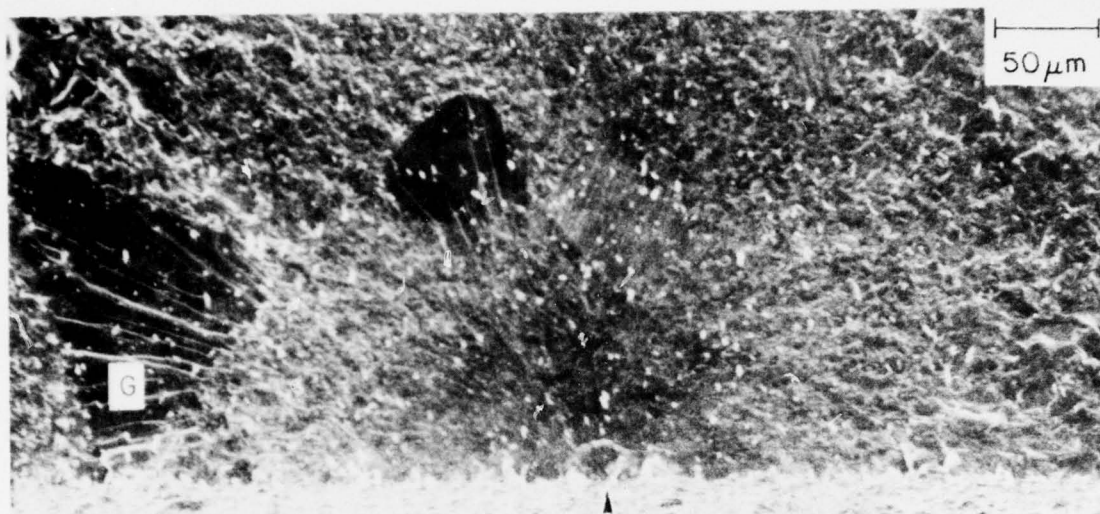


Figure 2. Example of fracture not initiating from larger grains. This lower magnification photo of B_4C (the same specimen shown at higher magnification in the right hand portion of figure 4) shows large grains to the left of the machining flaw origin (arrow). The largest grain (G) despite almost reaching the tensile surface is clearly not the source of failure showing that larger grains, while often sources of failure, are not always such sources.

the author is reasonably consistent with this, possibly suggesting a transition at somewhat larger G . Also, it shows a larger transition and lower strengths for specimens ground perpendicular in comparison to those ground parallel to the tensile axis. Because of possible differing compositions, and more generally because internal stresses may alter the apparent fracture energies calculated from the flaw sizes, such analysis is not attempted here.

Consider now Al_2O_3 , one of the more extensively studied materials; i.e. see figures 5-7. Also note table 1 where much of the machining and mechanical testing parameters for these and other studies are given. Figure 5 shows earlier Al_2O_3 data of various investigators each indicating to various degrees, a S-G transition as expected. More recent flexural data of Al_2O_3 (fig. 5) again indicates various transitions, e.g. at larger G for specimens ground perpendicular than for those ground parallel to the tensile axis. Figure 7 represents various data from diametral compression tests of Al_2O_3 with indicated specimen compositions and sizes. While clearly significant less certain because of the limited data, these results are again consistent with a S-G transition. Note that all of the Al_2O_3 transitions are reasonably consistent, especially when one considers the uncertainty of the G values due to exaggerated grain growth. More specifically, they are also consistent with flaws observed in single and polycrystalline Al_2O_3 , e.g. figure 9.

Consider next, BeO , one of the more extensively studied ceramics after Al_2O_3 . Note that the extensive studies of carefully characterized material by Fryxell and Chandler [27] clearly suggest a transition at $G \sim 25 \mu m$ (fig.7). While this data is corrected to zero porosity (P), the individual sets of samples of \sim constant porosity each show similar trends. Also, this corrected data agrees well with the data of Bentle and Kniefel [28] for hot pressed BeO with $P \sim 0$. Note that Greenspan's incomplete data [30] would suggest a possible transition at finer G , which is consistent with the fact that his specimens were probably ground approximately parallel with the tensile axis while those of Fryxell and Chandler, and Bentle and Kniefel, were circumfer-

TABLE 1
MACHINING AND FLEXURE TEST DATA

		Flexure Test				
Investigator	Machining	Specimen (GM)		Type ²	Span(s) (cm)	LR ³ (mm/min)
		Cross Sect.	Length			
A. Al ₂ O ₃ :						
Spriggs & Vasilos	G (30 μ in)	0.38x 0.63	4.45	4	3.80 1.27	~ 0.15?
Passmore et al	G (ER ~ 0.4mm) then an. 24hr 900°C	0.38x 0.63	4.45	4	3.80 1.27	
Rice	G(320 grit) ER	0.25x	1.5	3	1.27	1.27
Evans & Tappin	G, ER	0.5 0.4 x 0.5	2.5	3	2.0	0.051
Tressler et al	G various grits, (ER ~ 1/16", ~ 1.6 mm)	0.63 x 0.63	5.1	3	3.05	0.5
B. BeO:						
Fryxell & Chandler	CG rods	0.58(dia)	8.88	4	7.61 2.54	1.52
Veevers	G rods	0.41(dia)	2.54	4	1.90 0.79	0.76
Bentle & Kniefel	Core drilled rods	0.25(dia)	2.54	3	1.90	0.051
Greenspan	G(25-35 rms)	~0.7 x 0.7	> 5	3	5.08	1-2 min to failure
O'Neill & Livey	G?	~0.43 x 0.43	2.54	3	2.0	unspecified
Hill et al	G?	~0.43 x 0.43	2.54	3	2.0	
C. MgO:						
Evans & Davidge	Sawn	0.35x 0.45	2.6	4	2.4 1.2	0.051
Bradt et et al	D(C) G, ⊥ T.A. 100,220,400, or 600 grit	1.27x 1.27	3.8	3	3.05	0.51
Rice	G(320 grit), then DS (600 grit SiC) T.A., ER	0.25x 0.51		3	1.27 or 1.9	1.27
D. SiC:						
Gulden	3μ lapped (E.F.?)	.01x 0.1	< 0.63	4	0.43 .016	0.051
Cappola & Bradt	G?	0.64x 0.64	5.1	4	3.81 1.27	0.051
Prochazka & Charles	G(220 grit, 0.025mm per pass, 0.31 m/min EC)	0.254x 0.254	2.54	3	1.59	0.051

(continued)

TABLE 1

Investigator	Machining ¹	Flexure Test				
		Specimen (GM)		Type ²	Span(s) (cm)	LR ³ (mm/min)
		Cross Sect.	Length			
Cranmer et al	D(C) G \perp T.A. 220,320,400 or 600 grit (0.005 mm pass)	0.3x 0.3	3.0	3	19	0.051

¹All machining with diamond abrasive unless otherwise specified. G = ground, D(C)G = down (climb) ground, \perp or \parallel T.A. = perpendicular or parallel to tensile axis (i.e. bar length), ER = edges radius or rounding, EC = edges chamfered, EF = edge finishing; DC = dry sanded, an = annealed.

²3 point or 4 point flexure.

³LR = loading rate.

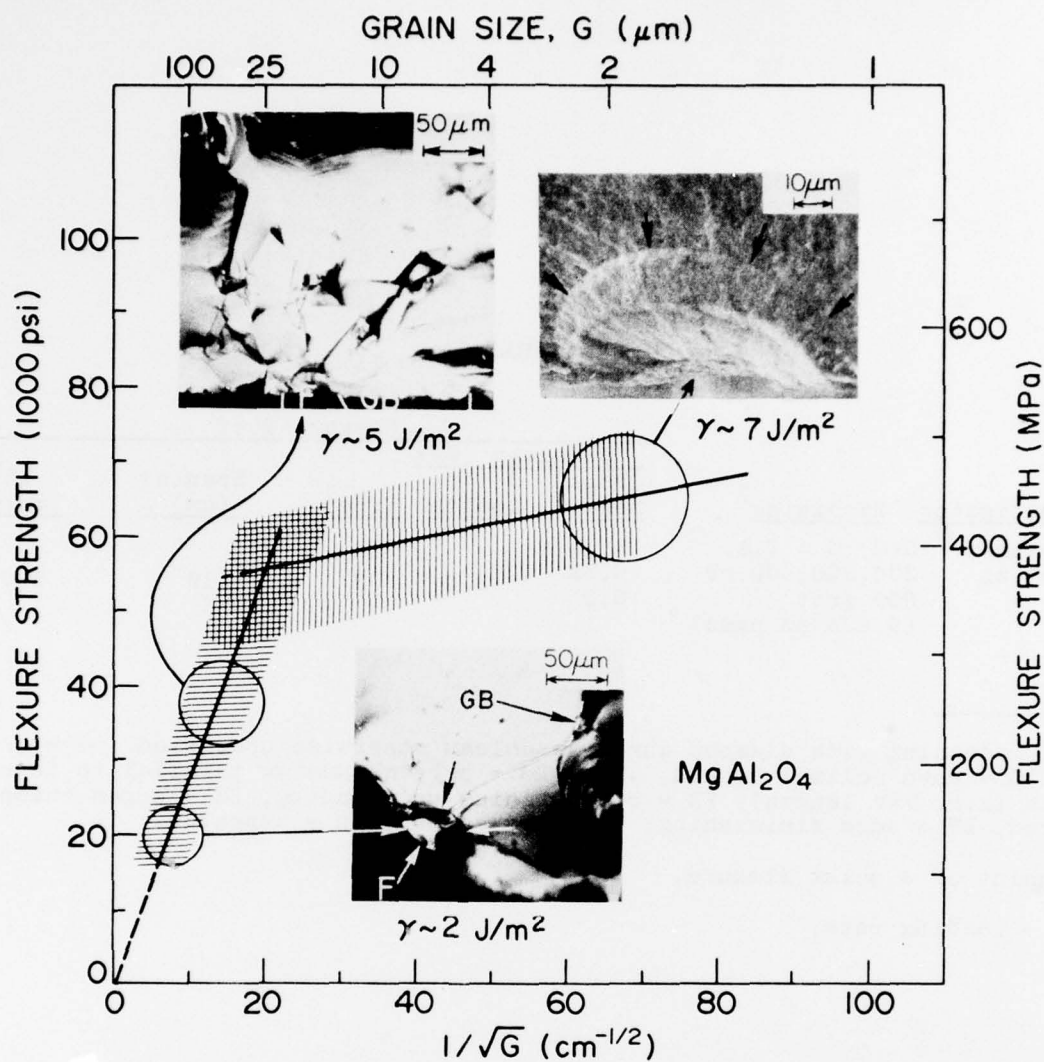


Figure 3. Strength-grain size behavior for MgAl_2O_4 . The crossed hatch region shows the extensive strength-grain size data for near theoretical density MgAl_2O_4 of good purity, as reported by Rice and McDonough [13]. Note the inserted fractographs showing flaws found at fracture origins for the indicated levels of strength. Also note the fracture energies calculated from the observed flaws show the transition from single to polycrystalline values as discussed in the text. Note that the flaw for the insert of intermediate strength consists of both a transgranular machining flaw portion, marked F, as well as a portion along the adjacent grain boundary, marked GB. Also note that the weaker orientation of single crystal specimens of the same size and surface finish as for the polycrystalline specimens give typical strengths of $\sim 210 \text{ MPa}$ (30,000 psi). The strength of polycrystalline specimens extends below this level.

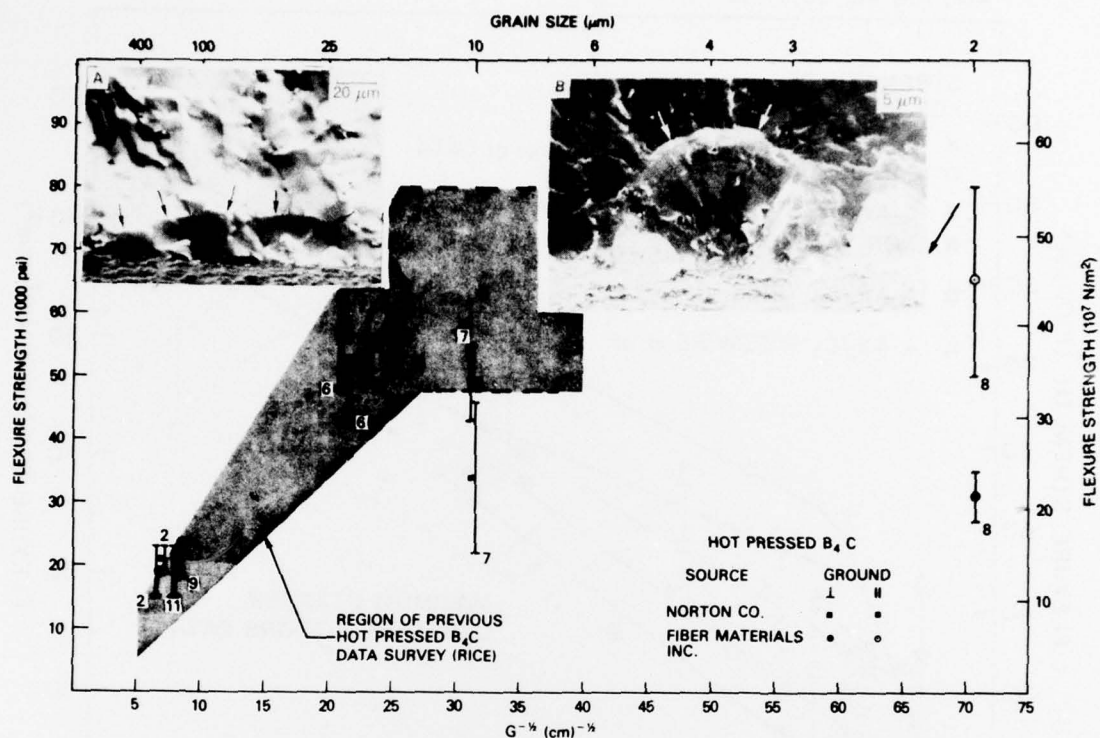


Figure 4. Strength-grain size data for hot pressed B_4C . Note the crossed hatch area representing analysis of an earlier survey of B_4C data [1], which gives a fair indication of S-G transition. More recent results of the author are shown by individual data points as well as the two fractograph inserts. The right insert shows a distinct fracture origin from a flaw much larger than the grain size in a fine grain body ground parallel with the tensile axis (see also fig. 2). The left insert shows a flaw whose depth is comparable to the intermediate grain size, but the flaw is fairly elongated perpendicular to the tensile axis. Internal stresses due to the non-cubic structure of B_4C as well as possible variations of stoichiometry in the different bodies makes fracture energy calculations from these flaw sizes and their interpretation in terms of the proposed fracture energy transition uncertain.

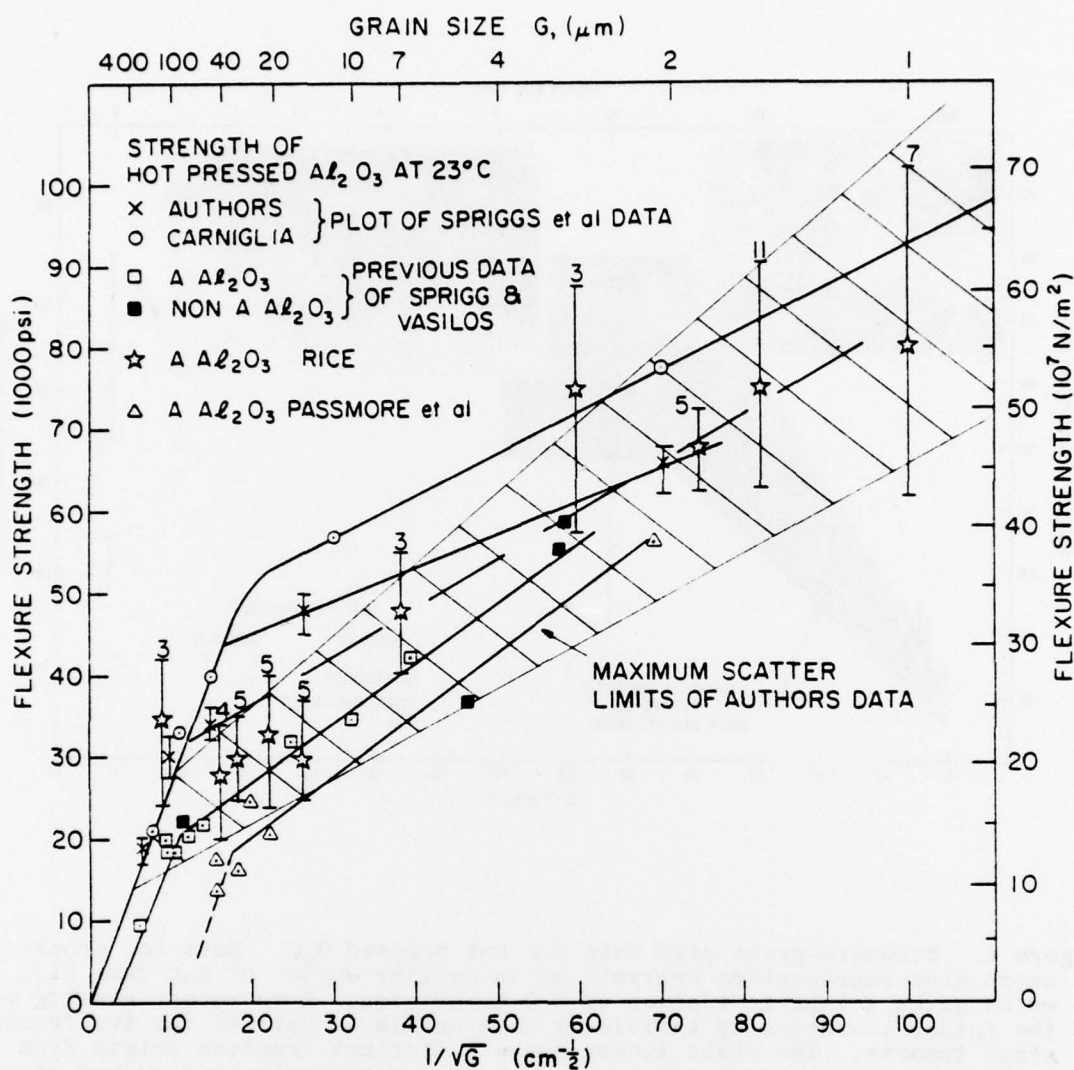


Figure 5. Earlier strength-grain size data for dense, machined Al_2O_3 . Note that while there are some differences in corrections for limited amounts of porosity, e.g. between Carniglia's and Rice's plot of Spriggs et al earlier data [1], all show strength-grain size transitions in the range of ~ 20 to $< 100 \mu\text{m}$. Note also that although specimens of Passmore et al [19] were annealed for 24 hours at 900°C after machining that both the fabrication temperature ($\geq 1400^\circ\text{C}$) as well as the temperature ($\sim 1700^\circ\text{C}$) for crack healing in larger grain Al_2O_3 [20] indicate that this annealing did not significantly effect the machining flaws.

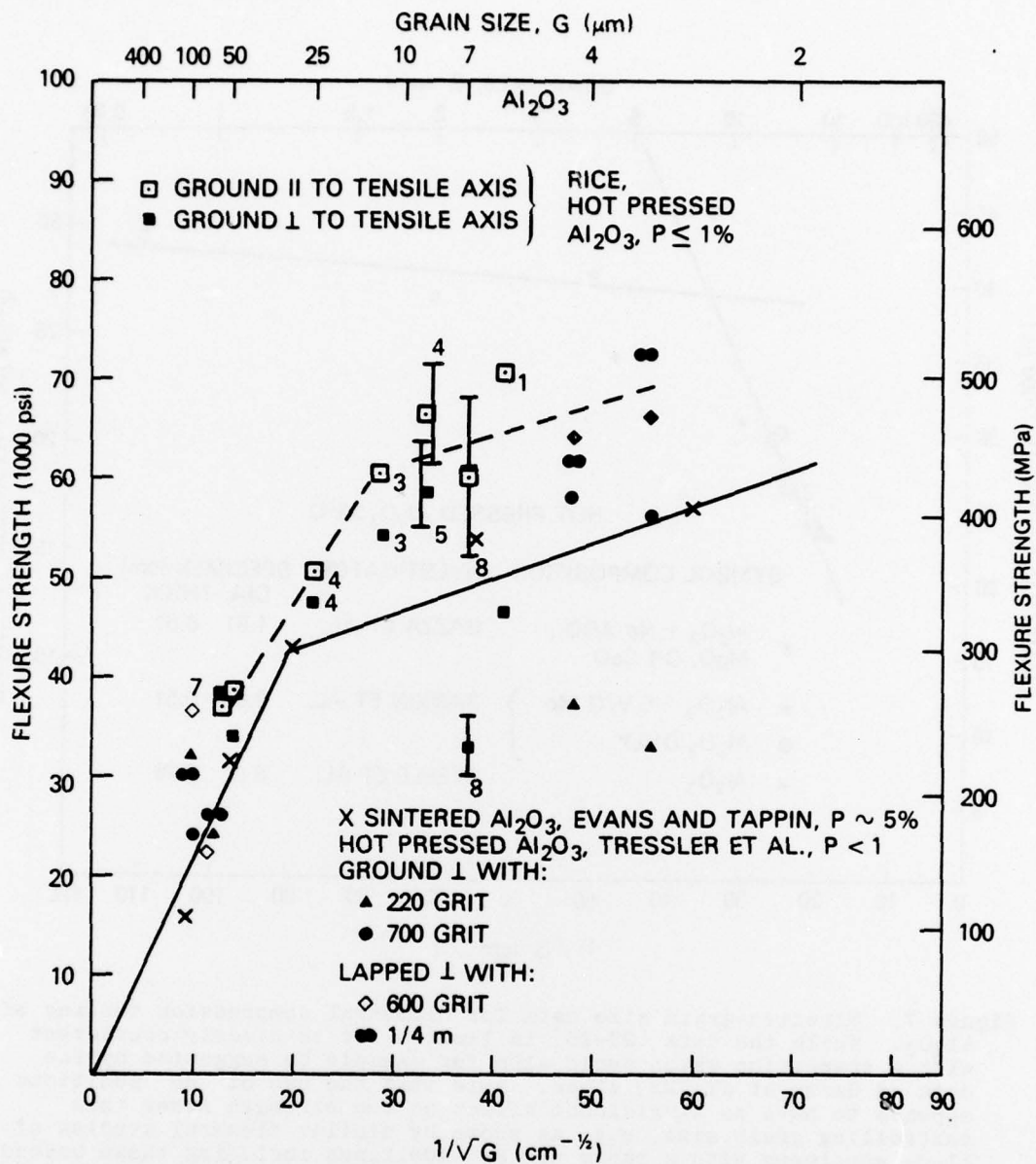


Figure 6. More recent strength-grain size data for Al_2O_3 . Limited data for parallel grinding, though scattered, shows a clear transition as does the limited data for perpendicular grinding, although this is more ill-defined [21]. Note that these transitions are reasonably consistent with the data of Evans and Tappin [22] for sintered alumina, especially when strengths are corrected for the $\sim 5\%$ porosity. Also note that the data for surface finishing of Tressler et al [7] with various grit sizes is consistent with the other data and the range of transitions that they indicate.

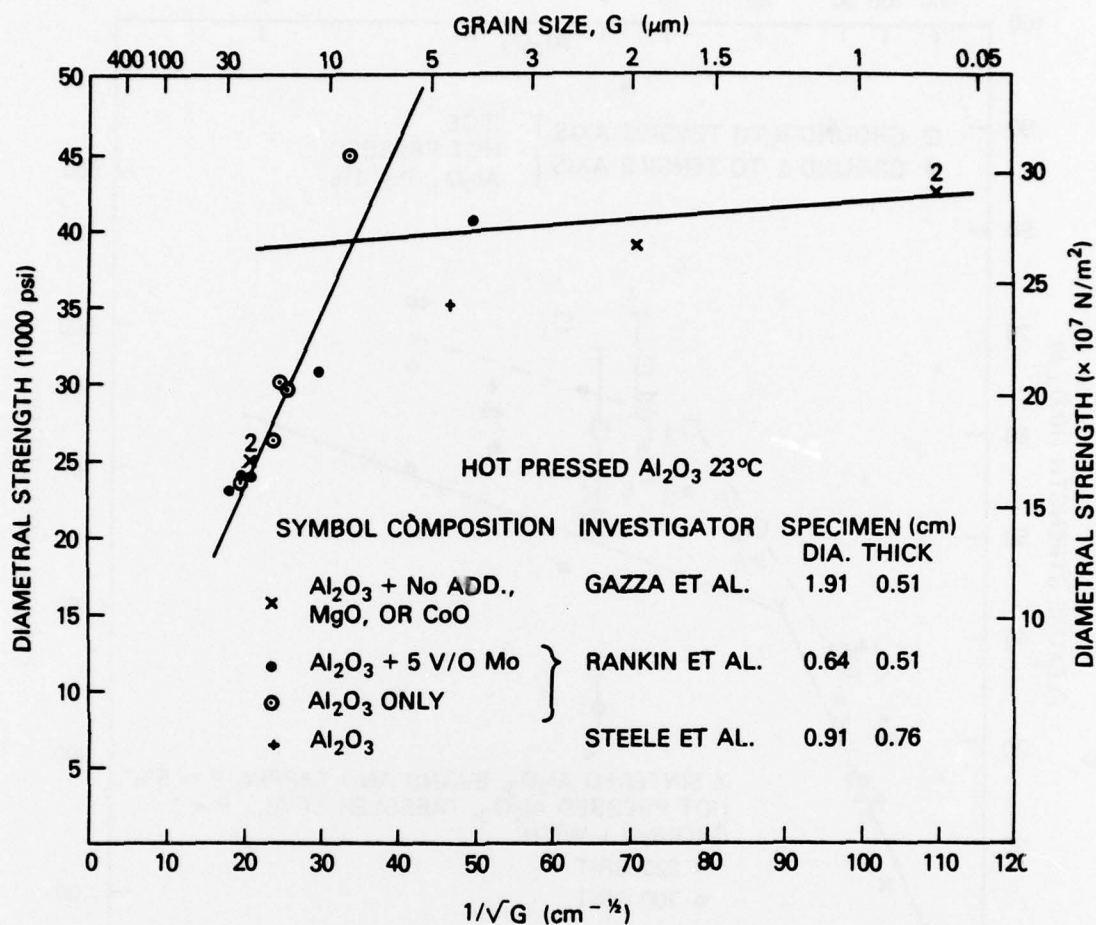


Figure 7. Strength-grain size data for diametral compression testing of Al_2O_3 . While the data [23-25] is limited, it is clearly consistent with a transition which would also for example be suggested by the data of Gazza et al [23] alone. Note that the use of Mo additions appears to have no significant affect on the strength other than controlling grain size, e.g. as shown by similar flexural studies of Al_2O_3 specimens with a range of Mo additions including those beyond the 5% level, by McHugh et al [26]. Note also that Rankin et al are the only ones to report a head travel rate (0.27 mm/min); however, Gazza (private communications) notes that they used the same head travel speed as Rankin et al. Steele et al's tests were conducted in a hand-operated press.

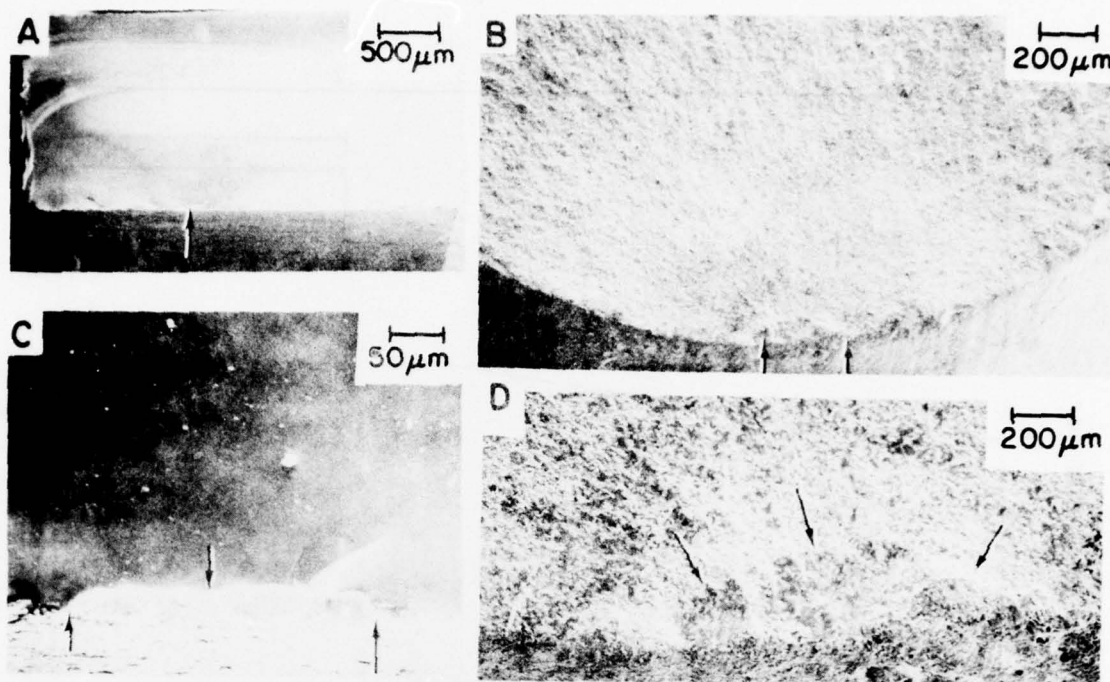


Figure 8. Example of machining flaws in Al_2O_3 . A and B) Machining flaw at the fracture origin of a sapphire laboratory test bar failing at 138 MPa (20,000 psi). C and D) Flaw at the fracture origin of a circumferentially machined large hot pressed Al_2O_3 tensile specimen having a gauge diameter of 14.4 mm, failure stress 275 MPa (40,000 psi). Note elongated flaws (arrows) due to machining perpendicular to the tensile axis in both samples.

entially machined. Also, Veavers' data [29], although low, in part due to its greater P , would also suggest a transition in the range observed for data of Fryxell and Chandler, and Bente and Kniefel, were it corrected to $P = 0$. Figure 10 presents more recent BeO data that suggests a transition at finer grain sizes in comparison with those of Fryxell and Chandler, and Bente and Kniefel. This is consistent with the data of figure 10 having higher strength expected from their probable grinding \sim parallel with the tensile axis.

An important question is whether the indicated C \sim G transitions for Al_2O_3 and BeO are due to machining or other flaws. In view of the densities and qualities of the bodies, dominance by processing flaws whose size is similar to machining flaws is unlikely. However, intrinsic flaws resulting from the TEA associated with their non-cubic crystal structures must also be considered. Data of Charles [33] on Lucalox rods with as-fired surfaces indicates a S-G transition at $G \geq 70 \mu\text{m}$. This is generally beyond the range of observed transitions for machined Al_2O_3 , but is in the G range for initiation of spontaneous cracks from TEA [34]. Similarly, Virkar and Gordon's S-G data on β - Al_2O_3 with as-annealed surfaces [35] shows a S-G transition at $G \geq 120 \mu\text{m}$. Though this value of G is probably somewhat high because of the tabular shape of the grains [4], the apparently similar thermal expansions and anisotropies of α and β aluminas again indicates that Al_2O_3 S-G transitions from intrinsic cracking are beyond those seen for the machined samples. This is also indicated by S-G data of as-annealed TiO_2 exhibiting spontaneous cracking and an associated S-G transition at $G \geq 50 \mu\text{m}$ [36],

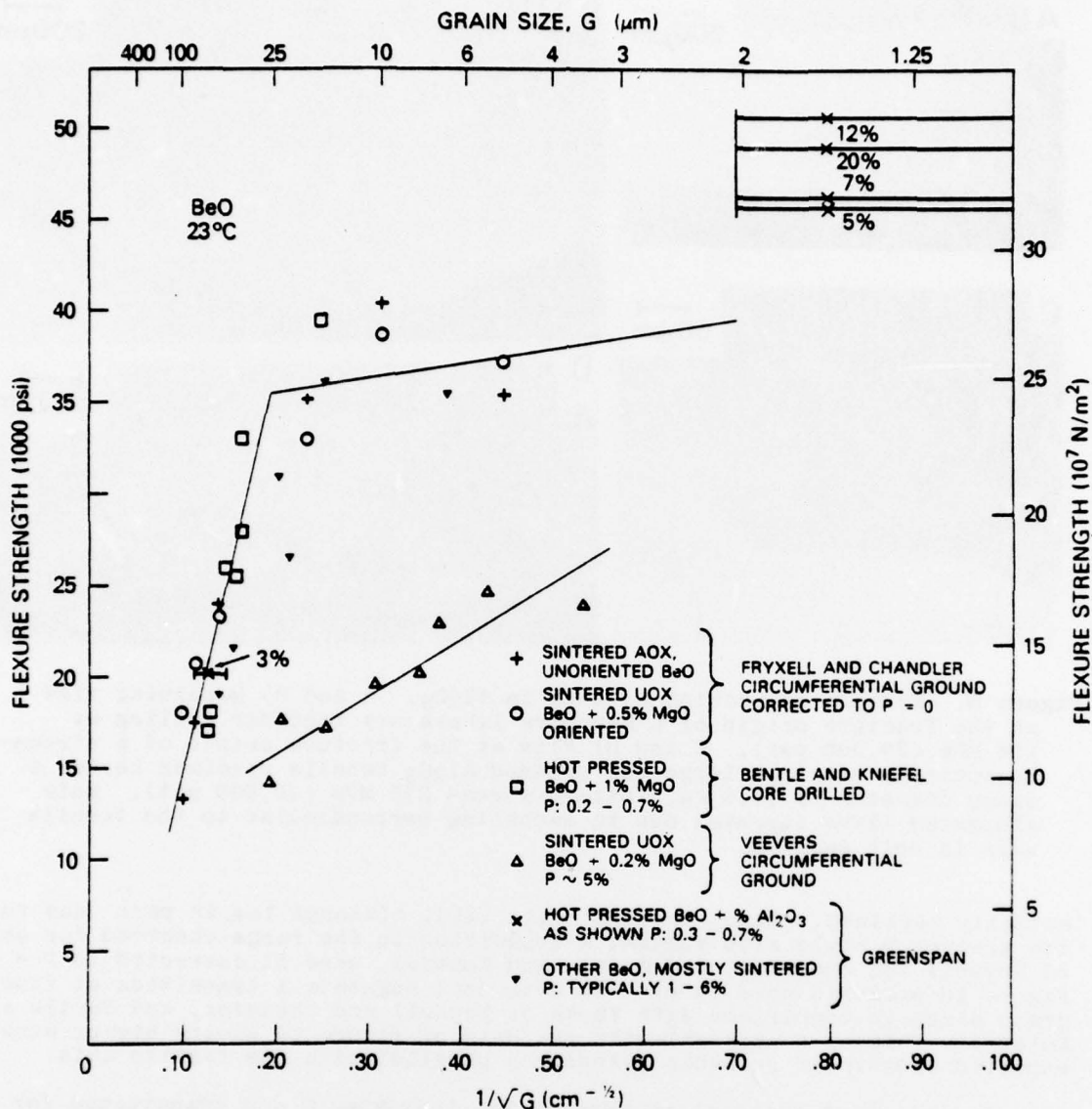


Figure 9. Strength-grain size data for earlier studies of BeO [27-30]. Note that the data of Fryxell and Chandler [27] is a compilation of their three sets of specimens having approximate constant porosities of 3.6, 8.6, and 13.6% all of which have been corrected to zero porosity using the porosity dependence determined by their study. Each of the individual sets of the specimens uncorrected for porosity would show approximately the same grain size transition. Note also that these corrected data agrees extremely well with hot pressed BeO of near zero porosity by Bentle and Kneifel [28].

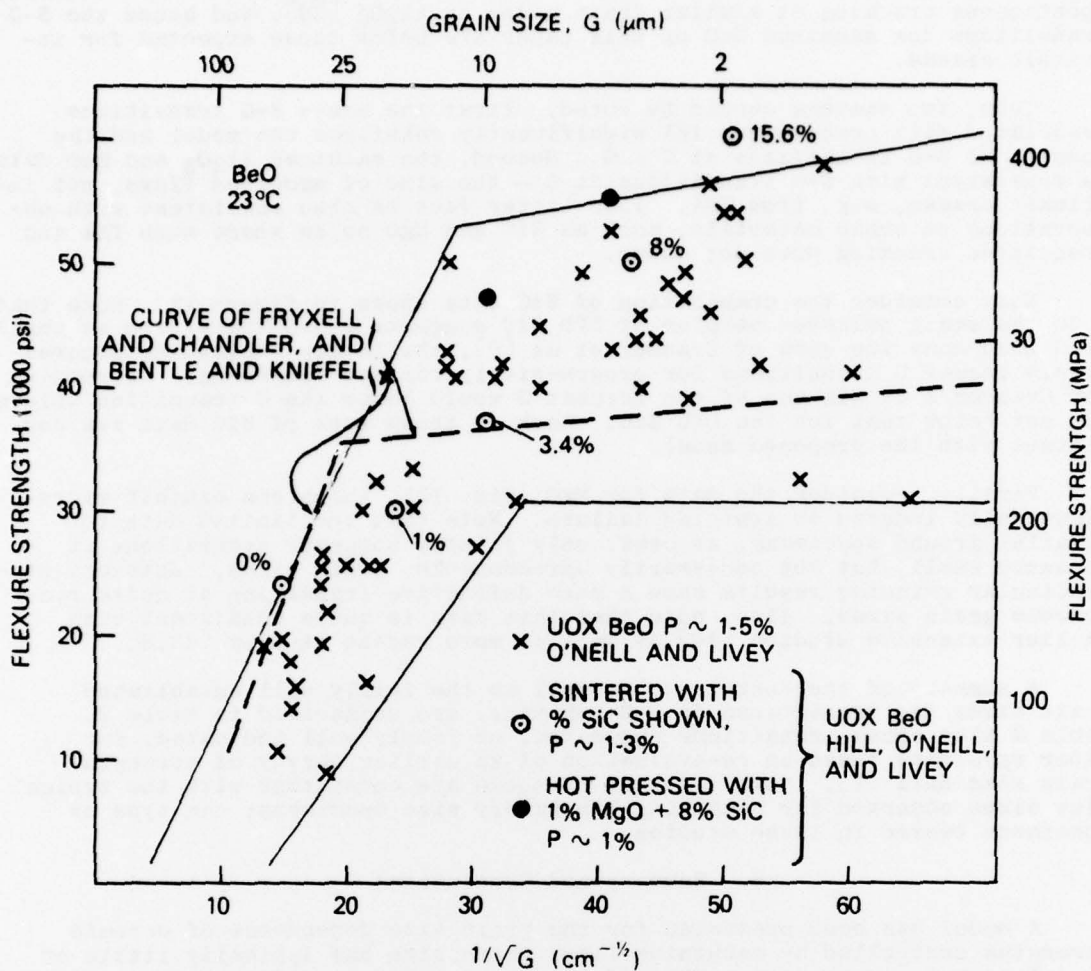


Figure 10. More recent strength-grain size data for BeO [31,32]. Note the distinct transition shown by the data of O'Neil and Livey [31] and that this transition is at a finer grain size than that indicated by data of Fryxell and Chandler, and Bentle and Kneifel. This is consistent with the proposed model since O'Neil and Livey's samples apparently were both smaller and were probably ground parallel with the tensile axis while those of all authors in figure 9, except probably Greenspan, were ground perpendicular to the tensile axis.

since TiO_2 exhibits such cracking at smaller G than Al_2O_3 [44]. BeO exhibits spontaneous cracking at similar grain sizes as Al_2O_3 [34], and hence the S-G transitions for machined BeO of this paper are below those expected for intrinsic cracks.

Thus, two factors should be noted. First the above S-G transitions associated with cracks from TEA significantly reinforce the model and the concept of S-G transitions at $C \sim G$. Second, the machined Al_2O_3 and BeO data is consistent with S-G transitions at $G \sim$ the size of machined flaws, not intrinsic cracks, e.g. from TEA. This latter fact is also consistent with observations on cubic materials, such as SiC and MgO below where such TEA and associated cracking does not occur.

Next consider the compilation of SiC data shown in figure 11. Note that both the small polished samples of CVD SiC suggests a S-G transition at smaller G than does the data of Cranmer et al [9], the latter indicating progressively larger G transitions for progressively coarser finishing. Correction for Cranmer's et al's use of the largest G would lower the G transition values, but not below that for the CVD SiC . Both of these sets of SiC data are consistent with the proposed model.

Finally, consider the data for MgO (fig. 12), which can exhibit microplastically induced or assisted failure. Note that the limited data for parallel ground specimens, at best, only faintly suggests transitions at somewhat small, but not necessarily unreasonable, grain sizes. However, perpendicular grinding results show a more definitive transition at quite reasonable grain sizes. Also, note that this data is quite consistent with earlier extensive studies [40] as well as more recent studies [42,8].

A summary of the tentative, as well as the fairly well established grain sizes for transitions in S-G behavior, are summarized in table 2. Table 2 also shows transitions suggested, or fairly well indicated, for other specimens based on re-evaluation of an earlier survey of strength grain size data [1]. Note that all of these are consistent with the typical flaw sizes observed for machining laboratory size specimens; the type of specimens tested in these studies.

5. Summary and Conclusions

A model has been presented for the grain size dependence of ceramic strengths controlled by machining flaws whose size has typically little or no relation to grain size. The model consists of two regimes. In the finer grain regime, flaws are substantially larger than the grain size so there is little or no decrease in strength with increasing grain size. Thus, strength-grain size curves are typically straight lines extrapolating to non-zero intercepts on a Petch ($S-G^{-1/2}$) plot.

In the larger grain regime, flaws are smaller than the grains and strengths decrease substantially with increasing grain size. When flaws are not too much smaller than G , e.g. $C > G/3$ subcritical growth to the grain size probably occurs. At small C/G ratios, e.g. $C/G < 1/3$ the fracture energies undergo a transition from grain boundary (for intergranular flaws) or single crystal (for transgranular flaws) to polycrystalline fracture energies as the flaw size to grain size ratio increases (mainly due to changing grain size). In any event, the transition between the finer and larger grain size regimes occurs when the flaw size (C) and grain size (G) are similar. Besides the smearing out of the transition in strength behavior due to C growing to G , the transition may not necessarily occur at $C = G$ for reasons such as flaw shape and location, as well as preferred grain orientation and the crystal orientation of fracture energy. Thus, an increase in flaw size shifts both the fine and large grain portions of the curves downward and increases the grain size of the transition between the two curves.

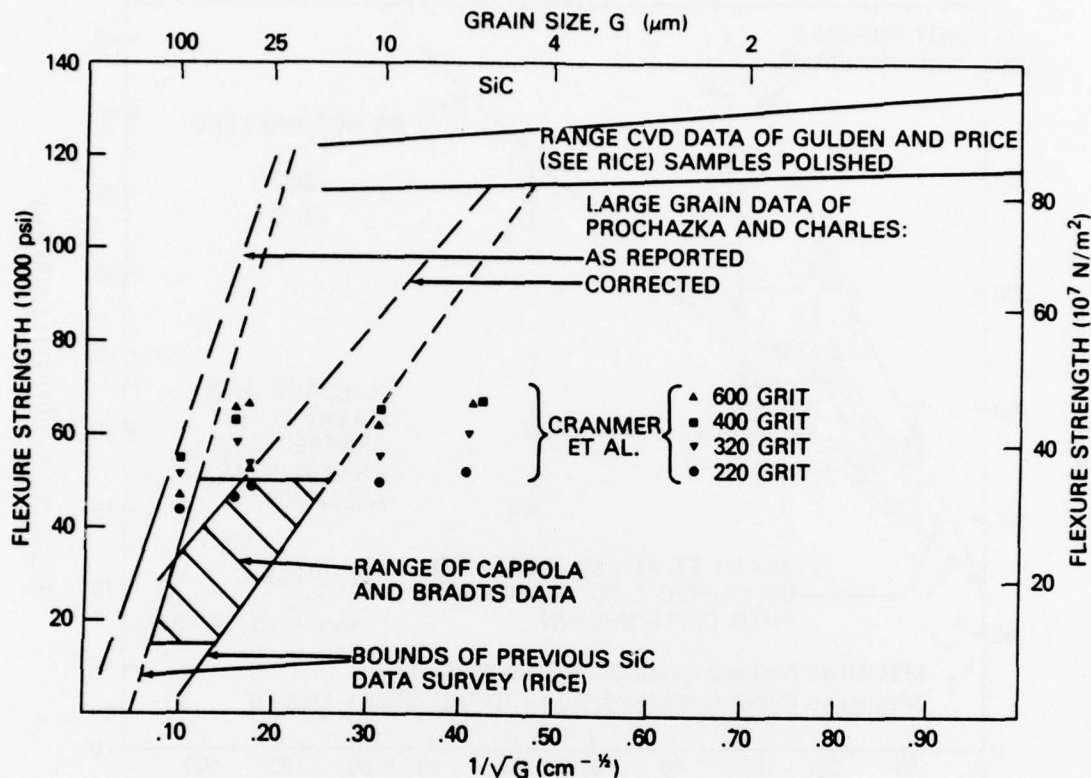


Figure 11. Strength-grain size data for SiC [1,4,6,9,37-39]. Note the consistency between the range of the previous data surveyed by Rice [1] and the more recent data of Coppola and Bradt [30]. Also note that these two ranges are more consistent with the correction of Prochazka and Charles [38] data as suggested by Rice et al [4]. These would suggest a transition for the small CVD SiC specimens of Gulden and Price from a few to ~ 20 microns. Note also the studies of hot pressed SiC ground or lapped perpendicular to the tensile axis with the various grit sizes [9] would indicate transitions at larger grain sizes. However, it should also be noted that Crammer et al plotted their data as a function of the largest grain size in the body. While larger grain sizes within a given body often mean the data should be represented by a somewhat larger grain size than the average, complete use of the largest grain size is probably an overcompensation (e.g. see fig. 2) so the G values for the transitions indicated by Crammer et al's data are probably somewhat high.

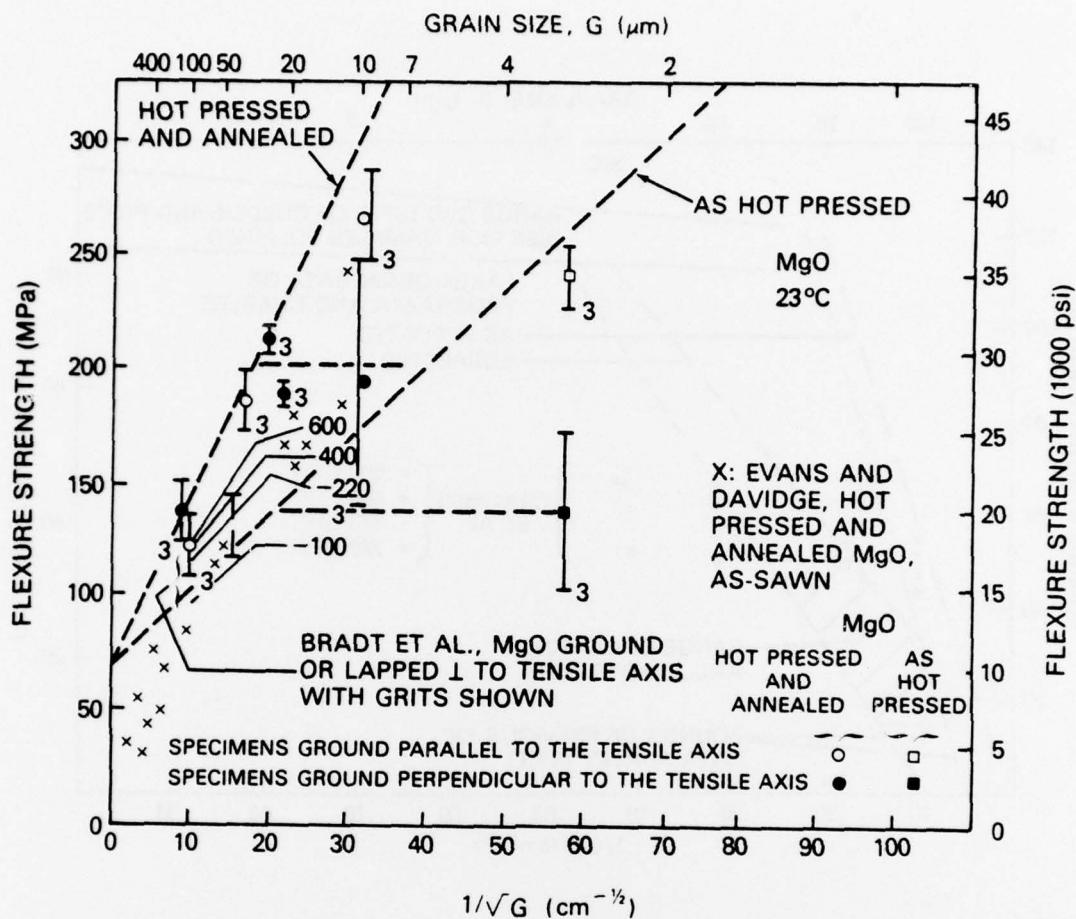


Figure 12. Strength-grain size data for MgO [8,21,40-42]. The dashed lines represent earlier extensive data of Rice [40]. Note that the more limited data for grinding parallel with the tensile axis [21,41] suggests that the transition for the as-hot pressed and hot-pressed, and annealed bodies at grain sizes from ~ 3 to $15 \mu\text{m}$. Note the earlier specimens of Rice [1] were tested with a 600 grit dry sanded surface for as-hot pressed samples while most of the hot pressed and annealed samples were tested with as-annealed surfaces. This more definitive indication of a transition in strength-grain size behavior for both types of samples ground perpendicular to the tensile axis and both of these transitions are clearly at larger grain sizes than those indicated for parallel ground samples. Note also the good agreement of the data of Bradt et al for samples ground or lapped perpendicular to the tensile axis with the various grit shown. Also, the data of Evans and Davidge [42] for hot pressed and annealed samples of MgO tested with as diamond-sawn surfaces, is also reasonably consistent with the other data, i.e. falling below the curve for hot pressed and annealed MgO tested with annealed or ground surfaces as expected.

TABLE 2
"PETCH PLOT" BRANCHING¹

Material	Processing ²	Machining ³	Grain Size (μm) ⁴ of Branching
Al ₂ O ₃	Hot Pressing	Various grinding and sanding	30-90
Al ₂ O ₃	Hot Pressing	grinding	~ 20
Al ₂ O ₃	Hot Pressing	⊥ grinding	30-50
Al ₂ O ₃	Sintering P ~ 5%	Grinding	20-25
Al ₂ O ₃	Hot Pressed	Grinding (500 grit?)	~ 8 ⁵
Al ₂ O ₃	Press Forged ⁶	Diamond Ground	~ 10
BeO	Sintered	Circumferential (i.e. ⊥) grinding	~ 25
BeO	Hot Pressed	Grinding (?)	~ 20
BeO	Sintered (P:1-5%)	Grinding (?)	10-25
BeO	Hot Pressed	Grinding (?)	~ 15?
MgO	Hot Pressed {	Grinding	~ 4??
		Grinding ⊥	~ 40
	Hot Pressed {	Grinding	~ 15?
	and annealed {	Grinding ⊥	~ 25
MgAl ₂ O ₄	Sintered and Hot Pressed {	P:0-2% Grinding	25 ± 10
TiB ₂	Hot Pressing	Unspecified machining	5 - 20
B ₄ C	Hot Pressing	Unspecified machining	15 - 20
B ₄ C	Hot Pressing	Grinding ⊥	~ 20
B ₄ C	Hot Pressing	Grinding ⊥	≥ 25?
SiC	CVD	Polishing	5 - 20
SiC	Hot Pressed	Grinding ⊥ (400 or 600 grit)	~ 35
SiC	Hot Pressed	Grinding ⊥ (320 grit)	> 35?
SiC	Hot Pressed	Grinding ⊥ (220 grit)	~ 50?

¹All data from flexure tests at room temperature except for two noted cases of Al₂O₃.

²Approximate % porosity P shown for some bodies. Typically hot pressed bodies had ~ 1% or less porosity.

³|| and ⊥ refer to direction of grinding relative to the tensile axis. ? indicates uncertainty in direction. Unspecified machining means samples were machined from larger pieces by unspecified processes which would most commonly be grinding, probably at or near || to the bar axis.

⁴Question marks indicate values indicated by limited data.

⁵From data for diametral compression at 23°C.

⁶From tests at - 196°C [1].

⁷Data corrected to zero porosity. Consideration of values at the different ~ constant levels of a few percent porosity would give similar results.

A survey of strength-grain size data shows good support for the model and the transition grain sizes most commonly $\sim 20\text{-}50\text{ }\mu\text{m}$, are typically consistent with commonly observed machining flaw sizes.

References

- [1] Rice, R. W., Strength/Grain-size Effects in Ceramics, Proc. British Ceramic Soc. [20], 205-257 (1972).
- [2] Rice, R. W., Microstructure Dependence of Mechanical Behavior of Ceramics, in Treatise on Materials Science and Technology, Vol. II, Properties and Microstructure, R. K. MacCrone, ed., 199-381 (Academic Press, Inc., New York, N.Y., 1977).
- [3] Rice, R. W., Fractographic Identification of Strength-Controlling Flaws and Microstructure, Fracture Mechanics of Ceramics, Vol. 1, R. C. Bradt, D.P.H. Hasselman, and F. F. Lange, eds., 323-345 (Plenum Pub. Corp., New York, N.Y., 1974).
- [4] Rice, R. W., Freiman, S. W., Pohanka, R. C., Mecholsky, Jr., J. J. and Wu, C. Cm., Microstructural Dependence of Fracture Mechanics Parameters in Ceramics, Fracture Mechanics of Ceramics, Vol. 4, R. C. Bradt, D.P.H. Hasselman, and F. F. Lange, eds., 849-876 (Plenum Pub. Corp., New York, N.Y., 1978).
- [5] Rice, R. W. and Mecholsky, Jr., J. J., The Nature of Strength Controlling Machining Flaws in Ceramics, this conference.
- [6] Bradt, R. C. and Tressler, R. E., Microstructure/Surface Finish Control of the Strength of Polycrystalline Ceramics, Proc. of 6th Int. Mat. Symp. Ceramic Microstructures-76, R. M. Fulrath and J. A. Pask, eds., 785-795 (Westview Press, Boulder, Colorado, 1976).
- [7] Tressler, R. E., Langensiepen, R. A., and Bradt, R. C., Surface-Finish Effects on Strength-vs-Grain Size Relations in Polycrystalline Al_2O_3 , J. Am. Ceram. Soc. [57] 5, 226-227 (1974).
- [8] Bradt, R. C., Dulberg, J. L., and Tressler, R. E., Surface Finish Effects and the Strength-Grain Size Relationship in MgO , Acta Metallurgica [24], 529-534 (Pergamon Press, Great Britain, 1976).
- [9] Cranmer, D. C., Tressler, R. E., and Bradt, R. C., Surface Finish Effects and the Strength-Grain Size Relation in Sic, J. Am. Ceram. Soc. [60] 5, 230-237.
- [10] Rice, R. W., The Effect of Grinding Direction on the Strength of Ceramics, The Science of Ceramic Machining and Surface Finishing, NBS Special Publication 348, S. J. Schneider and R. W. Rice, eds., 365-376 (Govt. Printing Office, Wash., D. C. 20402, 1972).
- [11] Rice, R. W. and Freiman, S. W., The Grain Size Dependence of Fracture Energy in Ceramics, submitted for publication.
- [12] Rice, R. W., Pohanka, R. C. and McDonough, W. J., The Effect of Stresses from Thermal Expansion Anisotropy, Phase Transformations and Second Phases on the Strength of Ceramics, submitted for publication.
- [13] Rice, R. W. and McDonough, W. J., Ambient Strength and Fracture Behavior of MgAl_2O_4 , in Mechanical Behavior of Materials, Proc. of 1971 Int. Conf. on Mechanical Behavior of Materials, Vol. 14, 422-431 (The Society of Materials Science, Japan, 1972).

- [14] Rice, R. W., Freiman, S. W. and Mecholsky, Jr., J. J., The Dependence of Strength Controlling Fracture Energy on the Flaw Size to Grain Size Ratio, submitted for publication.
- [15] Singh, J. P., Virkar, A. V., Shetty, D. K. and Gordon, R. W., On Strength-Grain Size Relationships in Polycrystalline Ceramics, submitted to J. Am. Ceram. Soc.
- [16] Rhodes, W. H., Berneburg, P. L., Cannon, R. M. and Steele, W. C., Microstructure Studies of Polycrystalline Refractory Oxides, Summary Report, 29 March 1972 to 28 April 1973, prepared for U.S. Naval Air Systems, Contract No. N00019-72-C-0298.
- [17] Emrich, B. R., Technology of New Devitrified Ceramics - A Literature Review, Technical Documentary Report No. ML-TDR-64-203, Air Force Materials Laboratory Research and Technology Division, Air Force Systems Command, Wright-Patterson Air Force Base, Ohio (1964).
- [18] Stookey, S. D., Ceramics Made by Nucleation of Glass-Comparison of Microstructure and Properties with Sintered Ceramics, in Proc. Am. Ceram. Soc. Symp. on Nucleation and Crystallization in Glasses and Melts, 1-4 (1962).
- [19] Passmore, E. M., Spriggs, R. M. and Vasilos, T., Strength-Grain Size-Porosity Relations in Alumina, J. Am. Ceram. Soc. [48] 1, 1-7 (1965).
- [20] Lange, F. F. and Radford, K. C., Healing of Surface Cracks in Polycrystalline Al_2O_3 , J. Am. Ceram. Soc. [53] 7, 420-421 (1970).
- [21] Rice, R. W., Machining of Ceramics, in Ceramics for High-Performance Applications, Proc. of Second Army Materials Technology Conference, J. J. Burke, A. E. Gorum, and R. N. Katz, eds, 287-343 (Brook Hill Pub. Co., Chestnut Hill, Mass., 1974).
- [22] Evans, A. G. and Tappin, G., Effects of Microstructure on the Stress to Propagate Inherent Flaws, Proc. British Ceramic Soc., No. 20, 275-297 (1972).
- [23] Gazza, G. E., Barfield, J. R. and Preas, D. L., Reactive Hot Pressing of Alumina with Additives, Am. Ceram. Soc. Bull. [48] 6, 605-610 (1969).
- [24] Rankin, D. T., Stiglich, J. J., Petrak, D. R. and Ruh, R., Hot-Pressing and Mechanical Properties of Al_2O_3 with an Mo-Dispersed Phase, J. Am. Ceram. Soc. [54] 6, 277-281 (1971).
- [25] Steele, B. R., Rigby, F. and Hesketh, M. C., Investigations on the Modulus of Rupture of Sintered Alumina Bodies, Proc. British Ceramic Soc., No. 6, 83-94 (1966).
- [26] McHugh, C. O., Whalen, T. J. and Humenik, Jr., M., Dispersion-Strengthened Aluminum Oxide, J. Am. Ceram. Soc. [49] 9, 486-491 (1966).
- [27] Fryxell, R. E. and Chandler, B. A., Creep, Strength, Expansion, and Elastic Moduli of Sintered BeO As a Function of Grain Size, Porosity, and Grain Orientation, J. Am. Ceram. Soc. [47] 6, 283-291 (1964).
- [28] Bente, G. G. and Kniefel, R. N., Brittle and Plastic Behavior of Hot-Pressed BeO, J. Am. Ceram. Soc. [48] 11, 570-577 (1965).
- [29] Veevers, K., Recrystallization of Machined Surfaces of Beryllium Oxide, J. Australian Ceram. Soc. [5] 1, 16-20 (1969).

- [30] Greenspan, J., Development of a High-Strength Beryllia Material, Army Materials and Mechanics Research Center Report No. AMMRC-TR-72-16 (1972).
- [31] O'Neill, J. S. and Livey, D. T., Fabrication and Property Data for Two Samples of Beryllium Oxide, United Kingdom Atomic Energy Authority Research Group Report AERE-R4912 (1965).
- [32] Hill, N. A., O'Neill, J. S. and Livey, D. T., The Properties of BeO Containing up to 15 w/o SiC and up to 2 w/o MgO, Proc. British Ceramic Soc., No. 7, 221-232 (1967).
- [33] Charles, R. J., Static Fatigue: Delayed Fracture, in Studies of the Brittle Behavior of Ceramic Materials, Technical Report No. ASD-TR-628, 370-404, Aeronautical Systems Division, Wright Patterson AFB, Ohio (1962).
- [34] Rice, R. W. and Pohanka, R. C., The Grain Size Dependence of Spontaneous Cracking in Ceramics, accepted for publication in J. Am. Ceram. Soc. (1978).
- [35] Virkar, A. V. and Gordon, R. S., Fracture Properties of Polycrystalline Lithia-Stabilized β "-Alumina, J. Am. Ceram. Soc. [60] 1-2, 58-61 (1977).
- [36] Kirchner, H. P. and Gruver, R. M., Strength-Anisotropy-Grain Size Relations in Ceramic Oxides, J. Am. Ceram. Soc. [53] 6, 233-236 (1970).
- [37] Gulden, T. D., Mechanical Properties of Polycrystalline β -SiC, J. Am. Ceram. Soc. [52] 11, 585-590 (1969).
- [38] Prochazka, S. and Charles, R. J., Strength of Boron-Doped Hot-Pressed Silicon Carbide, Am. Ceram. Soc. Bull [52] 12, 885-891 (1973).
- [39] Coppola, J.A. and Bradt, R.C., Measurement of Fracture Surface Energy of SiC, J. Am. Ceram. Soc. [55] 9, 455-460 (1972).
- [40] Rice, R. W., Strength and Fracture of Hot-Pressed MgO, Proc. British Ceramic Soc., No. 20, 329-363 (1972).
- [41] Rice, R. W., The Effect of Grinding Direction on the Strength of Ceramics, in Proc. on the Science of Ceramics Machining and Surface Finishing, S. J. Schnieder, Jr. and R. W. Rice, eds., 365-376 (National Bureau of Standards Special Publication 348 (1972)).
- [42] Evans, A. G. and Davidge, R. W., The Strength and Fracture of Fully Dense Polycrystalline Magnesium Oxide, Phil. Mag. [20] 164, 373-388 (1969).